



## Improved Hand Vein Pattern Recognition using Genetic Algorithm

Mai M.Zidan<sup>1</sup> , Wael A.Mohamed<sup>1</sup> , Ashraf S.Mohra<sup>1</sup> , Khaled S.Ahmed<sup>1</sup> <sup>1</sup> Electrical Engineering Dept., Benha Faculty of Engineering- Benha University, Egypt Corresponding Author: first Author (e-mail:mai.abdelrasheed@bhit.bu.edu.eg).

### ABSTRACT

Hand-vein recognition is known for its high accuracy and stability among biometric modalities. The best aspect to optimize is likely feature selection, it is a continuous challenge in human recognition systems. Feature selection aims to limit the number of features and eliminate redundant data and noise, resulting in a high recognition rate. The goal of our proposed method is to extract new properties from the hand vein, such as vein direction, length, and joined veins, which are thought to be unique to a person. Filtering techniques as well as enhancement and segmentation algorithms were applied to the collected data. The study was divided into two parts: the first employed the "Hough transformation," which is used to extract structural information such as vein lengths and angles, and the second used the Genetic Algorithm (GA). Instead of employing a mutation process, the Genetic Algorithm (GA) was altered to use a levy search. The algorithm has been shown to be an effective method of computing when the search space is judged to be highly dimensional. A classifier that uses the K-nearest neighbor (K-NN) algorithm is employed to detect all correct characteristics. Several experiments were conducted on the extracted features, and the results revealed that this GA feature selection method can deliver excellent results with a small number of features. Finally, matching experiments were implemented for both parts, and the results obtained revealed that the second part yielded 100% accuracy compared to 99.5% reaching by traditional method.

**INDEX TERMS** Hand vein, Hough transformation, Genetic Algorithm (GA), K-nearest Neighbor (K-NN)

I. **INTRODUCTION** For a security access system, biometric feature authentication technology has been developed and implemented. Biometrics is a term used in computer science to describe the mathematical study of human characteristics such as fingerprints, palms, finger veins, eyes, voice, signature, gait, and DNA [1]. When compared to standard personal verification methods, such as passwords, PINS, magnetic

swipe cards, keys, and smart cards, which only provide limited security and reliability because biometric features are difficult to fake and very simple to employ, biometric feature authentication technology provides a more dependable and secure performance [2]. According to previous research, biometric traits such as fingerprints, iris, and face, are currently used in biometric recognition and do not provide a highly safe environment. The



fingerprint might be made with a gelatin mold to deceive the fingerprint reader, and the brightness of the environment will alter the detection of the iris pattern as well as the different views of the face captured, making it more difficult to recognize a face [3]. Because of their physiological qualities, which are unique, universal, and immune to impostor attacks, biometric identification systems based on dorsal hand vein patterns have received considerable attention in recent years [4]. With an increasing emphasis on security, automated personal identification using hand Vein biometric feature is becoming a very active topic in both research and practical applications. So we present a biometric authentication system for high security physical access control based on dorsal hand vein patterns.

## II. RELATED WORKS

One of the vascular patterns at the back of the hand is the dorsal vein. Owing to this property, the dorsal hand vein is difficult to injure, wear, copy, or counterfeit because it is located beneath the skin [5,6]. In addition, the dorsal hand vein is thought to be unique to each individual, with twins even having different vein patterns [5]. The dorsal hand vein provides enhanced security in the biometric recognition system compared with the fingerprints, iris, and face. Imaging sensors such as complementary metal-oxide-semiconductor (CMOS) or charge-coupled device (CCD) cameras, scanners, and webcams with the aid of an infrared source or a neutral density filter have been suggested in previous studies [2,7- 12]. However, other researchers opted to use reliable databases such as the dorsal hand vein image database from [13], the hand dorsal vein database from the North China University of Technology (NCUT) [14], the general primary data source (GPDS) [15], and the Bosphorus Hand Vein Database [16,17]. Obtaining an area of interest (ROI), enhancing, and denoising images are required during the image pre-

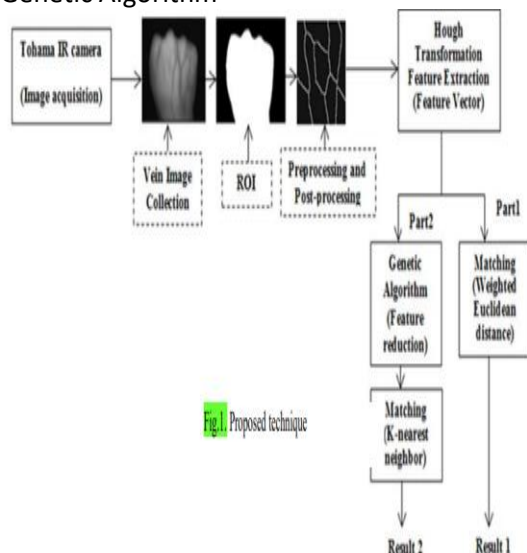
processing stage for the vein pattern to be easily spotted during the next segmentation stage. To extract the ROI of the dorsal hand vein, some researchers have used algorithms such as inventing datum points [2], Knuckle extraction [2,11,18], and gray normalization approaches [10]. Histogram equalization approaches such as contrast limited adaptive histogram equalization (CLAHE) [19], adaptive histogram equalization (AHE) [11,20,21], and equalized histogram [4] are among the techniques used to improve the ROI. Meanwhile, to minimize noise in the image, the researchers have used the Mai M.Zidan , Wael A.Mohamed1 , Ashraf S.Mohra1 , Khaled S.Ahmed1 1 Electrical Engineering Dept., Benha Faculty of Engineering- Benha University, Egypt Corresponding Author: first Author (e-mail: mai.abdelrasheed@bhit.bu.edu.eg ). 2 Wiener filter, smoothing filter, median filter, and 2-D Gaussian filter [3, 22-24]. A thresholding strategy, such as local dynamic or adaptive threshold with morphological operation [4,9,24,25], was developed to segment out the dorsal vein patterns from the image. Binarization was also advocated in [16], as it divides the ROI into white and black portions, with the black portion serving as the background. A local binary pattern (LBP) has been recommended in previous studies to extract the properties of the dorsal hand vein pattern [3,5,10]. LBP is a basic yet effective texture operator that labels the pixels of images by thresholding each pixel's neighborhood and treating the output as a binary number. Classification is required to identify the class of photos in a biometric recognition system. The winner-takes-all rule [6] states that the value "1" denotes the proper class, while "0" denotes the erroneous class, and the cross-entropy error is employed to determine inaccuracies. Previous studies have employed the Knearest neighbor (K-NN), support vector machine (SVM), random forest



[26], and Mahalanobis distance [25] to identify images. Although various strategies for dorsal hand vein detection have been developed, a more accurate system is required. This is because, according to a recent study, the accuracy of the existing approach is limited to 51-98 % or a 2-49 % error range. As a result, the goal of this research is to perform dorsal hand vein pattern recognition using HT characteristics to construct a dorsal hand vein authentication system using Genetic Algorithm (GA), and to assess the system's performance accuracy. III. MATERIALS AND METHODS For image collection, preprocessing, feature extraction, and classification, most hand-vein biometric systems use high-level architecture modules. The first portion of the study used the "Hough transformation" to extract structured data, such as vein lengths and angles from the investigated images, which were then categorized using Weighted Euclidean distance. The second half, on the other hand, employed the Genetic Algorithm (GA) to reduce the number of features after employing the Hough transformation feature and classified them using the K-nearest neighbor method (K-NN). The proposed hand dorsal vein recognition model for the input photos is shown in "Fig. 1." A. Image acquisition We used a newly designed box for the Image Acquisition stage of this model. We have designed a box for constraining the person's hand; it is suitable for the right and left hand. The box has a top opening for the IR camera to be placed inside it and a front opening for the person's hand. The box has a tube that connects the sides of the box and a ring installed around the tube in a specific location so that in order to prevent any large translation or rotation of the person's hand. It contains also a support before the tube and after the opening through which the person enters his or her hand to keep the hand upright . The hardware setup proposed by our

model displayed in the "Fig. 2.", consists of a Tohama IR camera, that is sensitive to the near infrared spectrum and is connected to the laptop via the USB cable, an Easycap connector that connects the IR cam to our MATLAB user interface and the box that contains the hands of the person. In order to minimize the effect of the surrounding environment on the quality of images and increase the uniformity of the acquired image, the hand is placed inside a box with the camera attached to one side facing the opposite side of the box. A hole was cut into the top perpendicular to the position of the back of the person's hand inside the box. The goal was to insert a hand with the rest of the box closed to get a better shot. The box has two holes, the first one lies at the top of the box with a diameter of 9cm that contains the IR camera and the second one lies at the front of the box with a diameter of 9cm and the camera's distance from the hand is 15cm. The second hole is a circular hole where the person enters his hand for the acquisition process to occur. The box dimension is (30 x 20 x 20 cm). The hand is placed along the tube inside the box to ensure that it is in the same position every time it enters the box with a support to ensure there is no rotation of the hand. This simplifies the image recognition task by avoiding the preprocessing tasks related to the rotation and translation correction. After acquiring the images, they are transferred to a PC to be saved on a database and to be used in further processing. The image resolution used is 720 x 480 pixels. The hardware setup plays a very important part in the design of a hand vein recognition system. The most important attribute of the





camera used to acquire the images must be the response to near infrared radiation. Attributes like spatial resolution and frame rate are less important because the image must be still and the vein pattern details are detected at short distance even with low resolution cameras. The laptop was the main processing device for the detection system. The specifications are as follows: • Windows: Windows 7 ultimate Service Pack 1 (32bit) • Intel® Core™ i3 CPU M 370 @ 2.40GHzPAGE 45 • 4 Gb RAM • Intel® Graphics Media Accelerator



Fig.2. Proposed technique

For the image acquisition in this study. The box is used to confine a person's hand, it can be used on any person's right or left hand. The initial stage in evaluating the performance of the system was to create a hand-vein database with 100 registered people. Three separate acquisitions from each hand were needed at various times for each person in the database (two images to train / learn and

one image to test for each hand); therefore, six images (three for the left and three for the right hand) were acquired for each person. Each person's hand was treated as a separate user for testing purposes. The 100 registered individuals represent a database of 600 different templates as shown in Table

I.

Image/ Database	Involved of the data base	Out of data base
All images	600	30
Training	400	--
Testing	170	30

B. Preprocessing First, we convert the RGB image to gray, then from gray to binary, and trace the region boundaries in the binary image. The Region of Interest (ROI) of the photos was then extracted by converting the image to a binary image and constructing a mask. Binarization divides an image into two parts: the object (hand region) and backdrop. The technique used in the segmentation substage is an iterative method for calculating and setting an effective threshold for segmenting the image into two parts: hand and background is presented in “Fig. 3”. Enhancing the contrast of the image using contrast-limited adaptive histogram equalization (CLAHE) is the next step.

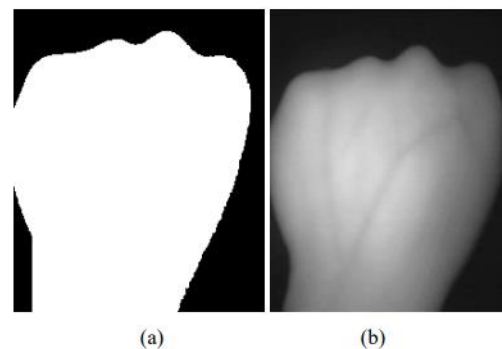
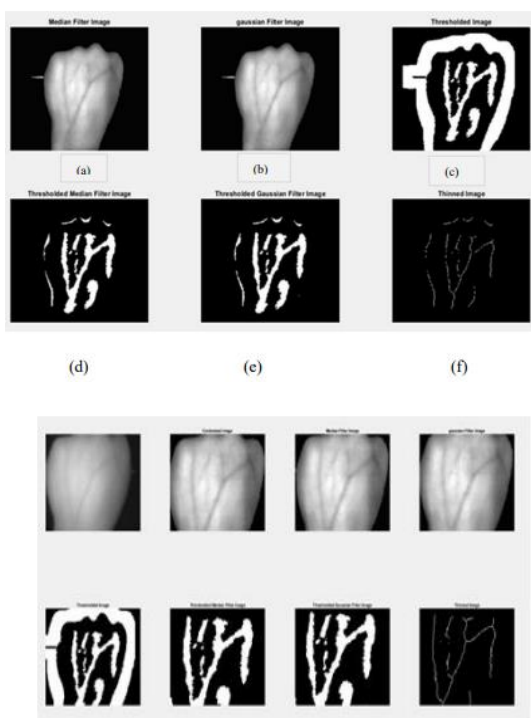


Fig 3: (a) Binary Mask (b) Extracted ROI

C. Smoothing and noise reduction The contrasted image was smoothed using a median filter, and any leftover noise was removed using a Gaussian filter. D. Post-processing A local adaptive threshold is



utilized to segment the filtered image. It is used to convert an image consisting of grayscale pixels to black and white scale pixels. Unlike the global thresholding technique, local adaptive thresholding chooses different threshold values for every pixel in the image based on an analysis of its neighboring pixels. Using the median filter and another Gaussian filter, the noise in the thresholded image was removed once again. Finally, morphological methods such as erosion and dilation are applied to the filtered image to obtain a thinned image as shown in Fig. 4.



(g) Fig. 4. (a) Median Filtered Image, (b)Gaussian Filter image, (c)Thresholded Masked Image, (d)Thresholded Median Filter Image, (e) Thresholded Gaussian Filter Image ,(f)thinning image and (g)pre-processing and post-processing for other data image. IV. FEATURE EXTRACTION AND CLASSIFICATION STAGE In this section, two algorithms are employed. The Hough transformation, as well as a suggested feature extraction approach based on a genetic algorithm (GA). A. Hough

Transformation Hough transform is a linear transform that can be used to detect straight lines. The straight line in the picture space is defined as  $y = mx + b$ , and can be plotted for each pair of image locations  $(x,y)$ . The Hough transform considers the features of the straight line in terms of its polar coordinate pair, abbreviated  $r$  and  $\Theta$  (theta), rather than picture points. The distance between the line and the origin is represented by parameter  $r$ , and the angle of the vector from the origin to the closest point is represented by parameter. The equation for the line can be expressed using the following parameterization[9]:  $y = (-\cos \theta \sin \theta ) x + ( r \sin \theta )$  (1) this can be rearranged as  $r = x \cos \theta + y \sin \theta$  (2) Consequently, each line of the image can be associated with a pair  $(r,\theta)$  that is unique if  $\theta \in [0,\pi)$  and  $r \in \mathbb{R}$ . In a thinned vein image, the Hough transformation can locate straight lines. The aim of the proposed study is to identify a unique features which vary between every person. It presents the three main veins together with conducted angles. It defines these lines and separates the features in the vein image, providing the extremes of the spotted lines as output and determining the angle of the lines about the x-axes. This was done by extracting the examined lengths and angles by setting a threshold for vein lengths (a minimum of 30 connected pixels) and space (maximum of 10 pixels). We compared the obtained image with the template image. Using this procedure, as shown in Fig. 5 illustrates an

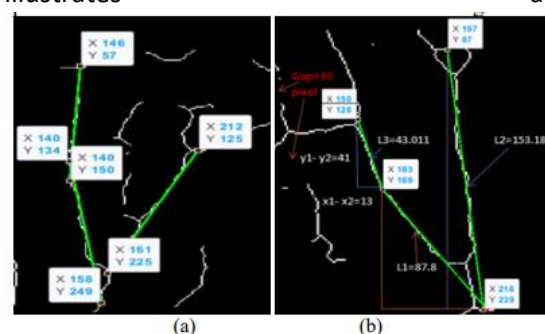


Fig. 5. (a),(b) Start and end points of each line



in vein image for samples of dataset. By calculating the vein lengths  $l_i$  via below "(3)",  $l_i = \sqrt{(x_{2i} - x_{1i})^2 + (y_{2i} - y_{1i})^2}$  (3) Where  $(x_1, y_1)$  and  $(x_2, y_2)$  are the start and end points of each straight line, respectively, and  $i$  is the number of straight lines in the vein image As example in Fig. 2 (a):  $l_1 = \sqrt{(146 - 140)^2 + (57 - 150)^2} = 93.1933$   $l_2 = \sqrt{(140 - 158)^2 + (150 - 249)^2} = 100.623$   $l_3 = \sqrt{(212 - 161)^2 + (125 - 225)^2} = 112.254$  And  $\theta_1 = 98^\circ$ ,  $\theta_2 = 105^\circ$ ,  $\theta_3 = 79^\circ$  We extract the start and end points of each line in the image using the Hough transformation, and then calculate the vein lengths (as  $l_1, l_2, l_3, \dots, l_i$ ) and angles between the veins and horizontal lines. Each image contained a varied number of lines/veins depending on the dataset. Consequently, we isolated three lines from the acquired image (right/left) and their associated angles to be studied, resulting in three vein lengths ( $l_1, l_2, l_3$ ) and three angles ( $\theta_1, \theta_2, \theta_3$ ) in each image. After the new estimated features of the investigated images were included, a new parameter (number of white pixels) was introduced to reflect the average brightness indicator of the image. When this parameter is combined with previously obtained data, each hand has seven distinct features that can be used in the classification stage. The weighted Euclidean distance is utilized to classify the Hough transformation's unique features (angle, length, and number of white pixels). It's utilized to categorize the unique element of a vein image that has to be recognized using the database's features. They are considered to belong to the same class when the gap between them is the shortest. This strategy was described in detail in my research, and this section is a follow-up to improve the output using another method[27]. Therefore, we used the GA to find the least feature(longest path and angle) by using six features from the Hough transform ( $l_1, l_2, l_3, \theta_1, \theta_2, \theta_3$ ). B. Proposed Genetic

Algorithm(GA) Feature Selection After extracting features from a vein image using the Hough transform, the proposed approach used a genetic algorithm for feature reduction. For feature subset selection using a genetic algorithm, the k-nearest neighbor approach must be utilized. As shown in Fig.6., genetic algorithms are part of a larger family of evolutionary algorithms that create solutions to optimization problems using natural evolution-inspired approaches such as mutation, selection, and crossover.

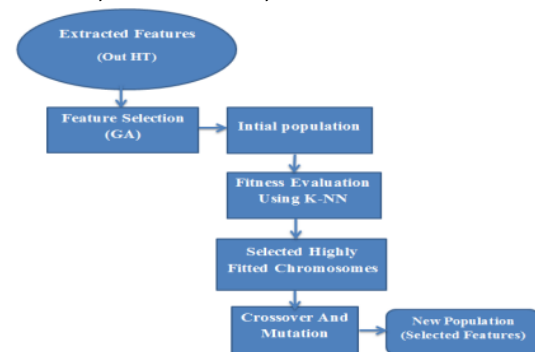


Fig.6. GA-Based feature Selection The characteristic selected is denoted by "1" on the first chromosome in the original population, while "0" indicates that the feature is not picked. Each chromosome has a value of "0" or "1" that indicates whether or not certain traits at a specific place are picked. The selected features are denoted by "1," and all the selected features have rankings; depending on these rankings, it is possible to develop new generations of children.

- Generation of Initial Population The initial population is first generated, and then the initial population of chromosomes is expressed in a bit string format. Each image generated six characteristics ( $l_1, l_2, l_3, \theta_1, \theta_2, \theta_3$ ) in this study (we took three images for each hand). Consequently, representing all chromosomal features in the search space is difficult. As a result, we created random chromosomes with a set length based on the size of our population. Individual population



fitness is assessed using an objective or fitness function in relation to certain criteria in this feature-selection problem[30].

- Fitness Evaluated Function Feature selection is required in a GA system to evaluate a proficient feature subset. To measure the fitness of each chromosome using a fitness function, a K-NN-based fitness function was employed for the GA because the K-NN algorithm is better at solving classification issues [29]. Here, k is determined by k number of features, and K-NN accuracy is obtained using the following formula:  $K\text{-NN accuracy} = x/d$  (4) Where x denotes the number of species photos in the set and d denotes the number of species accurately categorized. Following the evaluation of fitness assignment, new populations were created using crossover and mutation operators. It selects individuals who form the foundation of the following generation. These operators choose individuals based on their fitness levels. The optimization process has been stopped when the value of the fitness function for the best point in the current population is less than or equal to FitnessLimit.

- Crossover and Mutation Using the Darwin evolution concept, the genetic algorithm consists of three operators to generate new feature subsets: crossover, reproduction, and mutation. The likelihood of survival and fitness values of the chromosomes are proportional. Chromosomes with higher fitness values are more likely to participate in processes such as mutation and crossover. At the crossing point, two chromosomes are formed by swapping their parts. Bit strings were used to represent chromosomes in the GA. As a result, the GA can be used in the binary search space. Next, chromosomes will be rated among the top n elitist children to survive the next generation. The elite count identifier for elitism is always two [28]. The mutation operator causes the genes in each

chromosome to be disrupted, and this can be performed by flipping bits at random. We applied GA with K-NN to automatically discover the parameters of Squid species utilizing the crossover rate and mutation rate for this procedure to improve population diversity. For feature selection, we used a collection of hand-vein pictures. There were 100 patients in this study (with three images for each hand, total image=600 (400 for training, 200 for testing(containing 30 out of the data))). The parameter values used in the algorithms are as follows: m (chromosome length) = 170, maximum iteration = 1000, crossover rate (Pc) = 0.95, mutation rate (Pm) = 0.01, two-point crossover, elitist preserved model, N (population size) = 170, population type is bit string, m (chromosome length) = 400, maximum iteration = 1000, crossover rate (Pc) = 0.95, mutation rate (Pm) = 0.01, two-point crossover, and elitist preserved. The k value for the K-NN classifier is set at 100. V. CLASSIFICATION The fusion strategy between the structural features and brightness indication was evaluated using the weighted Euclidean distance. The minimum distance between the two analyzed photos (captured and template) can be used to determine whether the two images should be matched. In addition, K-NN was used to assess the GA approach. VI. EXPERIMENT RESULTS AND DISCUSSION After applying the gathered data to 600 photos, the results of the executed algorithms (fusion between structural features and brightness indication, GA) are discussed. The performance of the system was assessed using biometric performance metrics.

- Analysis and Evaluation To evaluate the performance of the established biometric system, the receiver operating characteristic (ROC) curve compares the false acceptance rate (FAR) to the genuine acceptance rate (GAR) (or 1 - False rejection rate (FRR)). The equal error rate (EER) was also used to



evaluate the performance. It is defined as the error rate when FAR and FRR are equal. A. False Acceptance Rate: The false acceptance rate (FAR) is a biometric accuracy metric that compares the total number of unauthorized people who gain access to the system with the total number of people who try to gain access. This denotes the likelihood that a biometric system will consider an inaccurate input to be a positive match. B. False Rejection Rate: The total number of authorized users not receiving access to the system, divided by the total number of people attempting to access the system, is known as the false rejection rate. The false rejection rate (FRR) is a measure of the likelihood that a biometric system will reject an input as a negative match when it is not. The features were retrieved using the Hough transformation approach, which had a 99.5 % accuracy rate. Table II. shows the FAR, FRR, and GAR results, where "Table III." shows the output of the Hough transformation obtained using this method ("Result found/Not" mean image in database or not) .

TABLE II: FAR, FRR, AND GAR OUTPUT

Number of Images	FAR (%)	FRR (%)	GAR (%)
10	0.200	0.100	0.900
20	0.100	0.050	0.950
30	0.066	0.033	0.967
40	0.050	0.025	0.975
200		0.005	0.995

TABLE III: THE OUTPUT OF HOUGH TRANSFORMATION

D. No.	Image No	L1	L2	L3	$\theta_1$	$\theta_2$	$\theta_3$	In dataset	Result found/Not
1	Name1_L	93.193	100.62	112.25	98	105	79	Yes	Found
2	Name2_L	87.8	153.18	43.011	173	142	162	Yes	Found
3	Name3_L	125.68	128.68	142.55	95.5	149	184.5	Yes	Found
4	Name4_L	124.98	90.118	129.082	127.5	182	176.5	Yes	Found
5	Name5_L	170.80	156.81	143.04	189	156	144	No	Found
...	...	...	...	...	...	...	...	...	...
49	Name49_L	170.9	111.45	92.4459	205	167	160	Yes	Not Found
50	Name50	143.04	158.08	112.591	190.50	193	-4.50	No	Found
...	...	...	...	...	...	...	...	...	...
200	Name200_L	184.07	116.40	92.2518	159	196.5	218	Yes	Found

D. No	Image No	Longest_L	$\theta$	In dataset	Result found/Not
1	Name1_L	112.254	79	Yes	Found
2	Name2_L	153.18	142	Yes	Found
3	Name3_L	142.55	184.5	Yes	Found
4	Name4_L	129.0827	176.5	Yes	Found
5	Name5_L	170.808	189	Yes	Found
...	...	...	...	...	...
49	Name49_L	170.808	205	Yes	Found
50	Name50	158.080	193	No	No Found
...	...	...	...	...	...
200	Name200_L	184.074	159	Yes	Found

TALBE V: FAR, FRR, AND GAR OUTPUT OF GA

Number of Images	FAR (%)	FRR (%)	GAR (%)
50	0.00	0.00	1.00
200		0.00	1.00

Features were retrieved using the GA approach, which had a 100% accuracy rate. Table IV. shows the output of GA(longest\_L,  $\theta$ ), whereas "Table V." displays the FAR, FRR, and GAR results obtained using the proposed technique

TALBE VI: Comparison of the proposed system with dorsal hand vein recognition system

Author/Year	Feature Extraction	Matching	System Results
Wang and Zheng 2018[34]	SIFT	Neighborhood structure, and the matching threshold	Ac=88.5%
Wan et. Al. 2017[11]	Caffe-Net, Alex-Net, and VGG-Net	Convolution neural network (CNN)	Ac=99%
Huang et al. 2016[36]	LBP+BC, and Graph	FGM	Ac=99.27%
Norah A. Al-johania and Lamiaa A. Elrefaei. 2019[35]	Caffe-Net, Alex-Net, and VGG-Net	ECOC with K-NN	Ac=90%
		ECOC with SVM	Ac=98.5%
		Transfer Learning	Ac=99.25%
Proposed method	Pixel-by-pixel	Correlation	Ac=98.5%
	Hough transformation	Angle, Length, and Weighted Euclidean	Ac=99.5%
	Hough transformation + Genetic Algorithm	K-NN	Ac=100%

VII. CONCLUSION Hand-vein patterns were employed in this study to identify people who





used a low-cost system. The system consisted of a black box with an arm for fixing the hand and a camera to capture photos that were connected to the PC. On 600 photographs obtained, a variety of advanced image processing algorithms were used (there are six images per individual in this data collection for 100 persons of varying ages and genders (three for the right hand and three for the left)). The data were used in two situations in the study. The first was to compare the tested image to the stored ones using the HT technique to extract structural features fused with brightness indicators to collect a collection of new features for the matching procedure. From each image, three lengths and three angles, as well as the number of white pixels, were retrieved and categorized using the Euclidean distance based on the retrieved features. It has 99.5 % accuracy, 0.05 % FAR, and 0.005 % FRR. The second method uses GA to extract features from images that have been categorized using K-NN. It provides 100 % accuracy, 0 % FAR, and 0 %FRR. When compared to the first technique, "HT," our proposed technique based on "GA" produced better results. And the total time is the time for HT ~ (62 secs) and time for GA ~0.8 sec(The total time of proposed method is ~63 secs but the computational time for some studies are not available). VII. Declarations A. Ethic's approval and consent to participate Not applicable. B. Consent for publication Not applicable. C. Availability of data and material The data that support the findings of this study are available on request from the corresponding author. D. Competing interests The authors declare that they have no competing interests. E. Funding This research received no specific grant from any funding agency in the public, commercial, or not-for-profit sectors. F. Authors' contributions The authors confirm contribution to the paper as follows: Khaled S.Ahmed conceived the experimental design

of the study. Mai M.Zidan developed the model, analyzed the data, and wrote the manuscript with support from Wael A.Mohamed, Khaled S.Ahmed. Ashraf S.Mohra had the supervision of the research. Mai M.Zidan, Khaled S.Ahmed contributed to the final version of the manuscript. E. Acknowledgements Not applicable.

**REFERENCES** [1] M. Singaram, P. Preveena, J. Sabitha and M. Shalini, " Dorsal Hand Vein Authentication System," International Journal of Innovative Research in Science, Engineering and Technology, vol. 8, pp. 2566-2571, 2019. [2] Y. Wang, K. Li and J. Cui, "Hand-dorsa Vein Recognition Based on Partition Local Binary Pattern," in International Conference on Signal Processing, ICSP 2010, IEEE, pp. 1671-1674, 2010. [3] M. M. N. M. Heenaye and R. K. A. Subramanian, "Study of Dorsa Vein Pattern for Biometric Security," University of Mauritius Research Journal. 2009, vol. 15, pp. 17-25, 2009. [4] Y. Wang, Y. Fan, W. Liao, K. Li, L. K. Shark and M. R. Varley, "Hand Vein Recognition Based on Multiple Keypoints Sets," 2012 5th IAPR International Conference on Biometrics, IEEE,. pp. 367-371, 2012. [5] K. Wang, Y. Zhang, Z. Yuan, and D. Zhuang, "Hand Vein Recognition Based on Multi Supplemental Features of Multi-Classifer Fusion Decision,"2006 IEEE International Conference on Mechatronics and Automation. IEEE, pp. 1790-1795, 2006. [6] M. Rajalakshimi, V. Ganapathy, and R. Rengaraj, "Palm-Dorsal Vein Pattern Authentication Using Convolution Neural Network (CNN)," International Journal of Pure and Applied Mathematics, vol. 116, pp. 525-532, 2017. [7] R. Raghavendra, J. Surbiryala, and C. Busch, "Hand Dorsal Vein Recognition: Sensor, Algorithms and Evaluation," 2015 IEEE International Conference on Imaging System and Techniques (IST), IEEE, pp. 1-6, 2015. [8] L. Chen, H. Zheng, L. Li, P. Xie, and S. Liu,



“Near-infrared Dorsal Hand Vein Image Segmentation by Local Thresholding Using Grayscale Morphology,” 2007 1st International Conference on Bioinformatics and Biomedical Engineering, IEEE, pp. 868-871, 2007. [9] P. Ramsiful and M. H. M. Khan, “Feature Extraction Technique for Dorsal Hand Vein Pattern,” Third International Conference on Innovative Computing Technology (INTECH 2013), IEEE, pp. 49-53, 2013. [10] A. Queslati, N. Feddaoui, and K. Hamrouni, “Identity Verification through Dorsal Hand Vein Texture Based on NSCT Coefficients,” 2017 IEEE/ACS 14th International Conference on Computer Systems and Application (AICCSA), IEEE, pp. 781-787, 2018. [11] S. Bhosale, and M. R. Jadhav, “Dorsal Hand Vein Pattern Recognition System Based on Neural Network,” 2017 International Conference of Electronics, Communication and Aerospace Technology (ICECA). IEEE, pp. 52-55, 2017. [12] P. Gupta, and P. Gupta, “Multibiometric Authentication System Using Slap Fingerprints, Palm Dorsal Vein and Hand Geometry,” IEEE Transactions on Industrial Electronics, vol. 65, pp. 9777-9784, 2018. [13] M. Shahin, A. Badawi, and M. Kamel. Biometric Authentication Using Fast Correlation of Near Infrared Hand Vein Patterns. International journal of biomedical sciences 2007. Vol. 2, no. 3, pp. 141-148, 2007. [14] X. Li, D. Huang, R. Zhang, Y. Wang, and X. Xie, “Hand dorsal vein recognition by matching Width Skeleton Models,” 2016 IEEE International Conference on Image Processing. (ICIP), IEEE, pp. 3146- 3150, 2016. [15] A. H. H. Alasadi and M.H. Dawood, “Dorsal hand-vein images recognition system based on grey level cooccurrence matrix and Tamura features,” International Journal of Applied Pattern Recognition, vol. 4, pp. 207-226, 2017. [16] B. Belean, M.Streza, S. Crisan, and S. Emerich, “Dorsal hand vein pattern analysis and Neural Network for biometric authentication system,” Studies in Informatics

and Control, vol. 26, pp. 305-314. 2017. [17] Bosphorus Hand Database. DotNetNuke Corporation. [2010; 2019 October 2], available from <http://bosphorus.ee.boun.edu.tr/hand/Home.aspx> [18] A. Kumar, and K.V. Prathyusha, “Personal authentication using hand vein triangulation and knuckle shape,” IEEE Transactions on Image Processing, vol. 18, pp. 2127-2136, 2009. [19] S. Kulkarni, and M. Pandit, “Biometric Recognition System based on Dorsal Hand Veins,” International Journal of Innovative Research in Science, Engineering and Technology, vol. 5, pp. 18899-18905, 2016. [20] R. Malutan, S. Emerich, S. Crisan, O. Pop, and L. Lefkovits, “Dorsal hand vein recognition based on Riesz Wavelet Transform and Local Line Binary Pattern,” 2017 3rd International Conference on Frontiers of Signal Processing (ICFSP), IEEE, pp. 146-150, 2017. [21] Z. Honarpisheh and K. Faez, “An efficient dorsal hand vein recognition based on firefly algorithm,” International Journal of Electrical and Computer Engineering (IJECE), vol. 3, pp. 30-41, 2013. [22] S. Sanchit, M. Ramalho, P. L. Correia, and L. D. Soares, “Biometric identification through palm and dorsal hand patterns,” 2011 IEEE EUROCON-International Conference on Computer as a Tool, IEEE, pp. 1-34, 2011. [23] S. Zhao, Y. Wang, and Y. Wang, “Extracting Hand Vein Patterns from Low-Quality Images: A New Biometric Technique Using Low-Cost Devices,” Fourth International Conference on Image and Graphics (ICIG 2007), IEEE, pp. 667-671, 2007. [24] D. Sandhiya and B. Thiyaneswaran, “Extraction of dorsal palm basilic and cephalic hand vein features for human authentication system,” 2017 International Conference on Wireless Communications, Signal Processing and Networking (WiSPNET), IEEE, pp. 2231-2235, 2018. [25] M. U. Akram, H. M. Awan, and A. A. Khan, “Dorsal hand vein based person identification,” 2014 4th International Conference on Image Processing Theory,



Tools and Applications (IPTA), IEEE, pp. 1-6, 2015. [26] Gopal, S. Srivastava, S. Bhardwaj, and S. Bhargava, "Fusion of palmphalanges print with palmprint and dorsal hand vein," Applied Soft Computing Journal, vol. 47, pp. 12-20, 2016. [27] M. M. Zidan, K. A. Mustafa, W. A. Mohamed and A. S. Mohra, "Hand Vein Pattern Enhancement using Advanced Fusion Decision," 2022 Advances in Science and Engineering Technology International Conferences (ASET), 2022, pp. 1-6, doi: 10.1109/ASET53988.2022.9734975. [28] Khare, P., Burse, K.: Feature selection using genetic algorithm and classification using weka for ovarian cancer. Int. J. Comput. Sci. Inf. Technol. 7(1), 194–196 (2016). ISSN 0975-9646. [29] Sangari Devi, S., Dhinakaran, S.: Crossover and mutation operations in GA-genetic algorithm. Int. J. Comput. Organ. Trends 3(4), 157–159 (2013). ISSN 2249-2593. [30] Zeng, D., Wang, S., Shen, Y., et al.: A GA based feature selection and parameter optimization for support tucker machine 111, 17–23 (2017)

